ANALI PAZU
Let. 15, Št. 1-2, pp. 19–42, november 2025

ANALI PAZU

SIMULACIJE DINAMIČNIH ODZIVOV ELEKTROMOTORSKIH POGONOV S TRIFAZNIMI ASINHRONSKIMI ELEKTROMOTORJI

RUDOLF PUŠENJAK

Rudolf Pušenjak, Fakulteta za industrijski inženiring Novo mesto, Slovenija
rudolf.pusenjak@fini-unm.si

DOPISNI AVTOR
rudolf.pusenjak@fini-unm.si

Sprejeto
29. 3. 2025

Recenzirano
10. 11. 2025

Izdano
28. 11. 2025

Znanstvena veda:
Tehnika

Članek predstavlja simulacije dinamičnih odzivov elektromotorskih pogonov s trifaznimi asinhronskimi elektromotorji v različnih motorskih, generatorskih in zavornih režimih delovanja. Za modeliranje elektromotorskih pogonov z asinhronskimi elektromotorji sta uporabljena splošni *qd*0 referenčni okvir in stacionarni referenčni okvir. Izpeljane so vodilne diferencialne in algebrajske enačbe asinhronskega stroja, ki so spojene z vodilnimi enačbami mehanskega bremena, pri čemer so matematični modeli obravnavanih elektromotorskih pogonov implementirani v programskem sistemu Mathematica®.

Ključne besede:
elektromotorski pogoni, asinhronski elektromotor, Parkova transformacija, referenčni sistem, delovni režimi pogonov

https://doi.org/10.18690/15.1-2.19-42.2025

Univerzitetna založba Univerze v Mariboru

ANALI PAZU
Vol. 15, No. 1-2, pp. 19–42, November 2025

ANALI PAZU

SIMULATIONS OF DYNAMICAL RESPONSES OF ELECTRIC MOTOR DRIVES WITH INDUCTION MACHINES

RUDOLF PUŠENJAK

Rudolf Pušenjak, Faculty of Industrial Engineering Novo mesto, Slovenia
rudolf.pusenjak@fini-unm.si

CORRESPONDING AUTHOR
rudolf.pusenjak@fini-unm.si

Accepted
29. 3. 2025

Revised
10. 11. 2025

Published
28. 11. 2025

The paper presents the simulations of dynamical responses of electric motor drives with induction machines working in various motor-, generator- and brake- regimes. For modeling of the electric motor drives with induction machines the arbitrary *qd*0 reference frame and stationary reference frame are used. The governing differential and algebraic equations of the induction machine are derived and coupled by the governing equations of the mechanical load, where the mathematical models of the entire drives are implemented in the programming system Mathematica®.

Science:
Technique

Keywords:
electric motor drives,
induction machine,
Park's transformation,
reference frame,
operation modes of
electric drive

University of Maribor Press

https://doi.org/10.18690/analipazu.15.1-2.19-42.2025

1 Introduction

The induction motors are converters of electrical energy into mechanical work, which by the development of power electronics became even more useful and are found in virtually all industrial areas of electric motor drives including rail vehicles [1] and electric vehicle drives [4]. They are rotating machines in which its rotor rotates at asynchronous speed and are characterized by simple construction, high efficiency, reliable operation in difficult conditions, minimal need for maintenance, low price and advanced speed control techniques.

The induction machine, used in electric motor drives can operate in three modes of operation: in motor, generator and brake mode, respectivelly. To enable dynamic simulation of drives with three-phase induction machines, the mathematical model in programming environment Mathematica® is developed in this paper. In addition, this software system uses symbolic computation capabilities, which allows the derivation of the governing equations of a three-phase induction machine, thereby saving a lot of laborious manipulation work. The paper is organized as follows. In the second chapter, using machine variables, the governing differential and algebraic equations of the three-phase induction machine are first written in vector form. These vector equations contain time-varying coefficients, which make their solution difficult. In order to facilitate the solution of these equations, the three-phase machine variables are decoupled using the Park's transformation into orthogonal two-phase q- and d- variables, so that the entire mathematical model is expressed in *qd*0 variables. The equations of the induction machine are supplemented with an equilibrium torque equation. In the third chapter, dynamic simulations of the electric motor drive with the selected type of induction machine are performed in all three operating modes. The final, fourth chapter provides conclusions.

2 Mathematical modeling of drives with three-phase induction machines

The term three-phase induction machine comes from the principle of operation, based on the Faraday's law of induction in which induced winding voltages are produced by the time changes of magnetic flux linkage created by the relative motion between stator and rotor windings and a spatially distributed magnetic field. In this article, the derivation of the mathematical model of a three-phase induction machine

will be performed for symmetrical machines, which consists of stator voltage equations, rotor voltage equations, flux linkage equations and torque equation. In machine variables, stator voltage equations take the vector form

$$\mathbf{v}_s^{abc} = \mathbf{r}_s^{abc}\mathbf{i}_s^{abc} + \frac{d}{dt}\boldsymbol{\lambda}_s^{abc}, \tag{1}$$

where $\mathbf{v}_s^{abc} = \left(v_{as}, v_{bs}, v_{cs}\right)^{\mathrm{T}}$ means the stator voltage vector in which the subscript *s* is referred to the stator, the upperscript *abc* is referred to the three phases of the machine and upperscript T denotes the vector transposition, $\mathbf{i}_s^{abc} = \left(i_{as}, i_{bs}, i_{cs}\right)^{\mathrm{T}}$ means the stator current vector of stator phases *abc*, $\boldsymbol{\lambda}_s^{abc} = \left(\lambda_{as}, \lambda_{bs}, \lambda_{cs}\right)^{\mathrm{T}}$ means the stator flux linkage vector and $\mathbf{r}_s^{abc} = r_s\mathbf{I}_3$ is the diagonal matrix of the ohmic resistances r_s of phase stator windings. Analogously, the rotor voltage equations in machine variables take the vector form

$$\mathbf{v}_r^{abc} = \mathbf{r}_r^{abc}\mathbf{i}_r^{abc} + \frac{d}{dt}\boldsymbol{\lambda}_r^{abc}, \tag{2}$$

where $\mathbf{v}_r^{abc} = \left(v_{ar}, v_{br}, v_{cr}\right)^{\mathrm{T}}$ means the rotor voltage vector in which the subscript *r* is referred to the rotor and upperscript *abc* is again referred to the three phases of the machine, $\mathbf{i}_r^{abc} = \left(i_{ar}, i_{br}, i_{cr}\right)^{\mathrm{T}}$ means the rotor current vector of rotor phases *abc*, $\boldsymbol{\lambda}_r^{abc} = \left(\lambda_{ar}, \lambda_{br}, \lambda_{cr}\right)^{\mathrm{T}}$ means the rotor flux linkage vector and $\mathbf{r}_r^{abc} = r_r\mathbf{I}_3$ means the diagonal matrix of the ohmic resistances r_r of phase rotor windings. The flux linkage equations for both stator and rotor of the magnetically linear machine can be presented in the coupled matrix form

$$\begin{pmatrix} \boldsymbol{\lambda}_s^{abc} \\ \boldsymbol{\lambda}_r^{abc} \end{pmatrix} = \begin{bmatrix} \mathbf{L}_{ss}^{abc} & \mathbf{L}_{sr}^{abc} \\ \mathbf{L}_{rs}^{abc} & \mathbf{L}_{rr}^{abc} \end{bmatrix} \cdot \begin{pmatrix} \mathbf{i}_s^{abc} \\ \mathbf{i}_r^{abc} \end{pmatrix}, \tag{3}$$

where $\mathbf{L}_{ss}^{abc}$, $\mathbf{L}_{rr}^{abc}$ are submatrices of stator-to-stator and rotor-to-rotor inductances

$$\mathbf{L}_{ss}^{abc} = \begin{bmatrix} L_{ls}+L_{ss} & L_{sm} & L_{sm} \\ L_{sm} & L_{ls}+L_{ss} & L_{sm} \\ L_{sm} & L_{sm} & L_{ls}+L_{ss} \end{bmatrix}, \quad \mathbf{L}_{rr}^{abc} = \begin{bmatrix} L_{lr}+L_{rr} & L_{rm} & L_{rm} \\ L_{rm} & L_{lr}+L_{rr} & L_{rm} \\ L_{rm} & L_{rm} & L_{lr}+L_{rr} \end{bmatrix}, \tag{4}$$

and where L_{ls}, L_{lr} are leakage inductances per phase of stator and rotor winding, respectively, L_{ss}, L_{rr} are self-inductances of stator and rotor winding, respectively and L_{sm}, L_{rm} are mutual inductances between stator windings and mutual inductances

between rotor windings, respectively. Further are $\mathbf{L}_{sr}^{abc}$, $\mathbf{L}_{rs}^{abc}$ submatrices of stator-to-rotor and rotor-to-stator mutual inductances, respectively. The stator-to-rotor mutual inductances are dependent on the rotor position, that is on the rotor angle θ_r between axes of phase *a* of stator and rotor winding, respectively, see Fig.1. Thus, submatrix $\mathbf{L}_{sr}^{abc}$ has the form

$$\mathbf{L}_{sr}^{abc} = \left[\mathbf{L}_{rs}^{abc}\right]^{\mathrm{T}} = L_{sr}\begin{bmatrix} \cos\theta_r & \cos\left(\theta_r + \frac{2\pi}{3}\right) & \cos\left(\theta_r - \frac{2\pi}{3}\right) \\ \cos\left(\theta_r - \frac{2\pi}{3}\right) & \cos\theta_r & \cos\left(\theta_r + \frac{2\pi}{3}\right) \\ \cos\left(\theta_r + \frac{2\pi}{3}\right) & \cos\left(\theta_r - \frac{2\pi}{3}\right) & \cos\theta_r \end{bmatrix}, \qquad (5)$$

where L_{sr} is the amplitude of the stator-to-rotor mutual inductance and where the superscript $^{\mathrm{T}}$ denotes the matrix transposition.

Substituting flux linkage vectors $\boldsymbol{\lambda}_s^{abc}$, $\boldsymbol{\lambda}_r^{abc}$ appearing in DEs (1) and (2) by matrix scalar products formed from the corresponding row of the inductance matrix in Eq. (3) with the assembled current vector, one obtain equations, which are coupled through mutual inductances between windings. Therefore, first-order DEs (1) and (2) are dependent on rotor position, too and by rotation of the rotor they are further dependent on the time. This creates differential equations with time-varying coefficients that are difficult to solve.

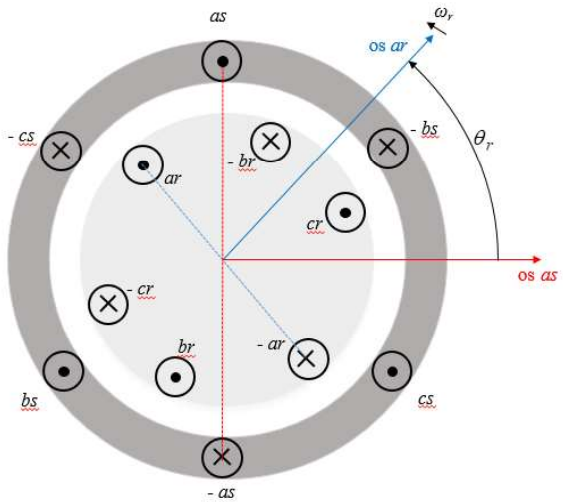

Figure 1: The angle θ_r between the axis of the phase *a* rotor winding and the axis of the phase *a* stator winding. Source: own.

2.1 The transformation to arbitrary *qd*0 reference frame

To circumvent difficulties due to the time-varying coefficients of mutual inductances and to decouple the three-phase machine variables to orthogonal two-phase (sometimes called two-axis) variables, the Park's transformation in arbitrary *qd*0 reference frame is applied. The *qd*0 transformation matrix has the form

$$\left[\mathbf{T}_{qd0}\left(\theta\right)\right]=\frac{2}{3}\begin{bmatrix}\cos\theta & \cos\left(\theta-\frac{2\pi}{3}\right) & \cos\left(\theta+\frac{2\pi}{3}\right)\\ \sin\theta & \sin\left(\theta-\frac{2\pi}{3}\right) & \sin\left(\theta+\frac{2\pi}{3}\right)\\ \frac{1}{2} & \frac{1}{2} & \frac{1}{2}\end{bmatrix} \tag{6}$$

and can be applied to transform voltages, currents or magnetic fluxes in *abc* machine variables to the *qd*0 variables by means of the transformation equation

$$\left(\mathbf{f}^{qd0}\right)=\begin{pmatrix}f^{q}\\ f^{d}\\ f^{0}\end{pmatrix}=\left[\mathbf{T}_{qd0}\left(\theta\right)\right]\cdot\begin{pmatrix}f^{a}\\ f^{b}\\ f^{c}\end{pmatrix}=\left[\mathbf{T}_{qd0}\left(\theta\right)\right]\cdot\left(\mathbf{f}^{abc}\right). \tag{7}$$

While the *q*- and *d*-components of Eq. (7) represent the decomposition of three-phase quantities into two orthogonal axes *q* and *d*, the third component, denoted by 0 is the zero-sequence component, which is added to enable the inverse transformation by means of the nonsingular transformation matrix $[\mathbf{T}_{qd0}(\theta)]^{-1}$. The geometric meaning of the relationship between *abc*-axes of a three-phase system and *q*- and *d*-axes of an arbitrary reference system is shown in Fig. 2.

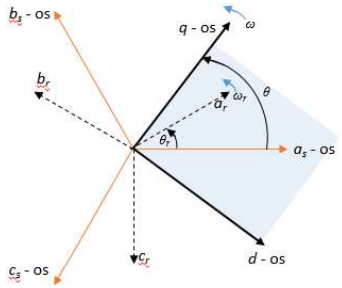

Figure 2: Relationship between *abc*-axes of a three-phase system and *qd*-axes of an arbitrary reference system. Source: own.

From Fig.2 it follows that the transformation angle $\theta(t)$ between q-axis of the arbitrary reference frame, which rotates at an arbitrary angular speed $\omega(t)$ and the a-axis, which corresponds to the stationary stator winding, varies according to the rule

$$\theta(t)=\int_0^t \omega(t)dt+\theta(0), \tag{8}$$

where $\omega(t)=d\theta/dt$. Analogously, the rotor angle $\theta_r(t)$ is measured between the stator and rotor a-phases and therefore varies as

$$\theta_r(t)=\int_0^t \omega_r(t)dt+\theta_r(0). \tag{9}$$

The angles $\theta(0)$ and $\theta_r(0)$ in Eqs. (8),(9) mean the corresponding initial values. The transformation of stator winding voltages (1) to the $qd0$ variables can be performed symbolically in Mathematica® programming environment. Let introduce matrices

$$\mathbf{r}_s^{qd0}=r_s\begin{bmatrix}1&0&0\\0&1&0\\0&0&1\end{bmatrix},\quad \mathbf{r}_r^{qd0}=r_r\begin{bmatrix}1&0&0\\0&1&0\\0&0&1\end{bmatrix},\quad \mathbf{E}=\begin{bmatrix}0&1&0\\-1&0&0\\0&0&0\end{bmatrix}, \tag{10}$$

and use the first and third matrix to derive the transformed voltages to the form

$$\mathbf{v}_s^{qd0}=\mathbf{r}_s^{qd0}\mathbf{i}_s^{qd0}+\frac{d}{dt}\boldsymbol{\lambda}_s^{qd0}+\omega\mathbf{E}\boldsymbol{\lambda}_s^{qd0}. \tag{11}$$

By using the programming environment Mathematica®, we can also derive symbolically the rotor winding voltages in $qd0$ variables. However, from Fig. 2 it follows, that transformation angle for rotor variables is equal to θ-θ_r, what implies the use of the transformation matrix $[\mathbf{T}_{qd0}(\theta-\theta_r)]$. Doing so, we get the following equation of rotor winding voltages in $qd0$ variables

$$\mathbf{v}_r^{qd0}=\mathbf{r}_r^{qd0}\mathbf{i}_r^{qd0}+\frac{d}{dt}\boldsymbol{\lambda}_r^{qd0}+(\omega-\omega_r)\mathbf{E}\boldsymbol{\lambda}_r^{qd0}, \tag{12}$$

where we use the second and third matrix (10).

The programming system Mathematica® proves to be very useful also in the symbolic derivation of flux linkage equations in terms of $qd0$ variables. From Eq. (3), the stator flux linkages in machine variables are given by $\boldsymbol{\lambda}_s^{abc}=\mathbf{L}_{ss}^{abc}\mathbf{i}_s^{abc}+\mathbf{L}_{sr}^{abc}\mathbf{i}_r^{abc}$ so that transformed equation looks like

$$\begin{aligned}\boldsymbol{\lambda}_s^{qd0}&=\left[\mathrm{T}_{qd0}(\theta)\right]\left(\mathbf{L}_{ss}^{abc}\mathbf{i}_s^{abc}+\mathbf{L}_{sr}^{abc}\mathbf{i}_r^{abc}\right)\\&=\left[\mathrm{T}_{qd0}(\theta)\right]\mathbf{L}_{ss}^{abc}\left[\mathrm{T}_{qd0}(\theta)\right]^{-1}\mathbf{i}_s^{qd0}+\left[\mathrm{T}_{qd0}(\theta)\right]\mathbf{L}_{sr}^{abc}\left[\mathrm{T}_{qd0}(\theta-\theta_r)\right]^{-1}\mathbf{i}_r^{qd0}\end{aligned} \tag{13}$$

The transformation (13) requires matrix multiplications involving the inverse transformation matrix, which can be easily obtained by symbolic.programming. The rotor flux linkages in machine variables are given by $\boldsymbol{\lambda}_r^{abc} = \mathbf{L}_{rs}^{abc}\mathbf{i}_s^{abc} + \mathbf{L}_{rr}^{abc}\mathbf{i}_r^{abc}$, which are transformed to the *qd*0 variables by transformation

$$\begin{aligned}\boldsymbol{\lambda}_r^{qd0} &= \left[\mathrm{T}_{qd0}(\theta-\theta_r)\right]\left(\mathbf{L}_{rs}^{abc}\mathbf{i}_s^{abc} + \mathbf{L}_{rr}^{abc}\mathbf{i}_r^{abc}\right) \\ &= \left[\mathrm{T}_{qd0}(\theta-\theta_r)\right]\mathbf{L}_{rs}^{abc}\left[\mathrm{T}_{qd0}(\theta)\right]^{-1}\mathbf{i}_s^{qd0} + \left[\mathrm{T}_{qd0}(\theta-\theta_r)\right]\mathbf{L}_{rr}^{abc}\left[\mathrm{T}_{qd0}(\theta-\theta_r)\right]^{-1}\mathbf{i}_r^{qd0}\end{aligned} \tag{14}$$

By assembling the computed results of Eq. (13) and of Eq. (14) together, the stator and rotor flux linkage equations in *qd*0 variables can be presented in the following explicit form

$$\begin{pmatrix}\lambda_{qs}\\ \lambda_{ds}\\ \lambda_{0s}\\ \lambda'_{qr}\\ \lambda'_{dr}\\ \lambda'_{0r}\end{pmatrix} = \begin{bmatrix} L_{ls}+L_m & 0 & 0 & L_m & 0 & 0\\ 0 & L_{ls}+L_m & 0 & 0 & L_m & 0\\ 0 & 0 & L_{ls} & 0 & 0 & 0\\ L_m & 0 & 0 & L'_{lr}+L_m & 0 & 0\\ 0 & L_m & 0 & 0 & L'_{lr}+L_m & 0\\ 0 & 0 & 0 & 0 & 0 & L'_{lr}\end{bmatrix}\begin{pmatrix}i_{qs}\\ i_{ds}\\ i_{0s}\\ i'_{qr}\\ i'_{dr}\\ i'_{0r}\end{pmatrix} \tag{15}$$

where the primed rotor variables are used for convenience and present the rotor values, recomputed to the stator side by means of the stator-to-rotor winding ratio:

$$\lambda'_{qr} = \frac{N_s}{N_r}\lambda_{qr},\quad \lambda'_{dr} = \frac{N_s}{N_r}\lambda_{dr},\quad i'_{qr} = \frac{N_s}{N_r}i_{qr},\quad i'_{dr} = \frac{N_s}{N_r}i_{dr},\quad L'_{lr} = \left(\frac{N_s}{N_r}\right)^2 L_{lr}. \tag{16}$$

while the magnetizing inductance L_m on the stator side is

$$L_m = \frac{3}{2}L_{ss} = \frac{3}{2}\frac{N_s}{N_r}L_{sr} = \frac{3}{2}\frac{N_s}{N_r}L_{rr}. \tag{17}$$

To complete the mathematical model of three-phase induction machine, we derive the torque equation in *qd*0 variables. For this purpose, we start with the sum of instantaneous input power of all six windings of the stator and rotor in machine variables and use the Park's transformation to obtain the corresponding expression in *qd*0 variables

$$
\begin{aligned}
p_{inp} &= v_{as}i_{as} + v_{bs}i_{bs} + v_{cs}i_{cs} + v'_{ar}i'_{ar} + v'_{br}i'_{br} + v'_{cr}i'_{cr} \\
&= \tfrac{3}{2}\left(v_{qs}i_{qs} + v_{ds}i_{ds} + 2v_{0s}i_{0s} + v'_{qr}i'_{qr} + v'_{dr}i'_{dr} + 2v'_{0r}i'_{0r}\right) \\
&= \tfrac{3}{2}\Big[r_s\left(i_{qs}^2 + i_{ds}^2 + 2i_{0s}^2\right) + r'_r\left(i'_{qr}{}^2 + i'_{dr}{}^2 + 2i'_{0r}{}^2\right) \\
&+ \frac{d\lambda_{qs}}{dt}i_{qs} + \frac{d\lambda_{ds}}{dt}i_{ds} + 2\frac{d\lambda_{0s}}{dt}i_{0s} + \frac{d\lambda'_{qr}}{dt}i'_{qr} + \frac{d\lambda'_{dr}}{dt}i'_{dr} + 2\frac{d\lambda'_{0r}}{dt}i'_{0r} \\
&+ \omega\left(\lambda_{ds}i_{qs} - \lambda_{qs}i_{ds}\right) + \left(\omega - \omega_r\right)\left(\lambda'_{dr}i'_{qr} - \lambda'_{qr}i'_{dr}\right)\Big]
\end{aligned}
\tag{18}
$$

The terms of the form ri^2 in Eq. (18) describe the copper loses and the terms of the form $(d\lambda/dt)i$ represent the rate of exchange of magnetic field energy between windings. Only terms of the form $\omega\lambda i$ describe the rate of energy, which can be converted to the mechanical work. Therefore, the developed electromechanical torque is defined as the sum of all $\omega\lambda i$ terms, divided by the rotor angular speed

$$
T_{em} = \tfrac{3}{2}\left(\frac{P}{2\omega_r}\right)\Big[\omega\left(\lambda_{ds}i_{qs} - \lambda_{qs}i_{ds}\right) + \left(\omega - \omega_r\right)\left(\lambda'_{dr}i'_{qr} - \lambda'_{qr}i'_{dr}\right)\Big], \tag{19}
$$

where $P/2$ denotes the number of pole pairs.

2.1.1 Mathematical model of induction machine in base quantities

In practice, we usually use magnetic flux linkages per second, denoted by Ψ instead of magnetic flux linkages λ and reactances x instead of inductances L. Denoting with $\omega_b=2\pi f$ the so called base angular frequency, the magnetic flux linkages per second and reactances, respectively are expressed by relations

$$
\Psi = \omega_b\lambda, \qquad x = \omega_b L\,. \tag{20}
$$

The introduction of magnetic flux linkages per second Ψ and reactances x, respectively, has a consequence that previously derived equations of mathematical model of the induction machine must be rewritten in terms of new variables. The stator voltage equation in $qd0$ variables is then rewritten into the form

$$
\mathbf{v}_s^{qd0} = \mathbf{r}_s^{qd0}\mathbf{i}_s^{qd0} + \frac{1}{\omega_b}\frac{d}{dt}\Psi_s^{qd0} + \frac{\omega}{\omega_b}\mathbf{E}\,\Psi_s^{qd0} \tag{21}
$$

and rotor voltage equation, in which variables are recomputed on the stator side, becomes

$$\mathbf{v}_r'^{qd0} = \mathbf{r}_r'^{qd0}\mathbf{i}_r'^{qd0} + \frac{1}{\omega_b}\frac{d}{dt}\Psi_r'^{qd0} + \frac{(\omega-\omega_r)}{\omega_b}\mathbf{E}\,\Psi_r'^{qd0}. \qquad (22)$$

Equation of flux linkages (15) now goes into equation of flux linkages per second:

$$\begin{pmatrix}\Psi_{qs}\\ \Psi_{ds}\\ \Psi_{0s}\\ \Psi'_{qr}\\ \Psi'_{dr}\\ \Psi'_{0r}\end{pmatrix} = \begin{bmatrix} x_{ls}+x_m & 0 & 0 & x_m & 0 & 0\\ 0 & x_{ls}+x_m & 0 & 0 & x_m & 0\\ 0 & 0 & x_{ls} & 0 & 0 & 0\\ x_m & 0 & 0 & x'_{lr}+x_m & 0 & 0\\ 0 & x_m & 0 & 0 & x'_{lr}+x_m & 0\\ 0 & 0 & 0 & 0 & 0 & x'_{lr}\end{bmatrix}\begin{pmatrix}i_{qs}\\ i_{ds}\\ i_{0s}\\ i'_{qr}\\ i'_{dr}\\ i'_{0r}\end{pmatrix}. \qquad (23)$$

Finally, the torque equation (19) is also rewritten in terms of magnetic flux linkages per second

$$T_{em} = \frac{3}{2}\left(\frac{p}{2\omega_r}\right)\left[\frac{\omega}{\omega_b}\left(\Psi_{ds}i_{qs} - \Psi_{qs}i_{ds}\right) + \left(\frac{\omega-\omega_r}{\omega_b}\right)\left(\Psi'_{dr}i'_{qr} - \Psi'_{qr}i'_{dr}\right)\right]. \qquad (24)$$

2.2 The transformation to stationary *qd*0 reference frame

The dynamic analysis of the induction machine together with its converter is in drives with adjustable rotor speed or in transient period more conveniently tractable in the stationary *qd*0 reference frame. The stationary reference frame is obtained from the arbitrary reference frame, when the angular speed ω is set to zero, ω=0. The compact vector form of a mathematical model of induction machine in the stationary *qd*0 reference frame then consists of the stator voltage equation:

$$\mathbf{v}_s^{qd0} = \mathbf{r}_s^{qd0}\mathbf{i}_s^{qd0} + \frac{1}{\omega_b}\frac{d}{dt}\Psi_s^{qd0}, \qquad (25)$$

rotor voltage equation:

$$\mathbf{v}_r'^{qd0} = \mathbf{r}_r'^{qd0}\mathbf{i}_r'^{qd0} + \frac{1}{\omega_b}\frac{d}{dt}\Psi_r'^{qd0} - \frac{\omega_r}{\omega_b}\mathbf{E}\,\Psi_r'^{qd0}, \qquad (26)$$

equation of flux linkages per second (23) and torque equation (24). It is again worth to mention that rotor voltage equation is expressed in primed variables, which all are recomputed on the stator side.

2.3 The torque balance equations of the electric motor drive

For simulation of the entire electric motor drive, the mathematical model of the induction machine must be completed with the torque balance equations, which take into account the mechanical load of the drive. If an electric motor drives a mechanical load through a gear transmission, the equilibrium state of the electric motor drive consists of two equations, where the first equation corresponds to the input side and the second to the output side of the gear transmission [2]. In this article, we will not discuss such drives, but will limit ourselves to direct drives, where the balance of the developed electromechanical torque and the mechanical load torque is described by a single equation. In such cases, the torque balance equation takes the following general form:

$$J\frac{d\left(\frac{2\omega_r}{P}\right)}{dt}=\left(\frac{2\omega_b}{P}\right)J\frac{d\left(\frac{\omega_r}{\omega_b}\right)}{dt}=T_{em}-T_{mech}-T_d\,, \qquad (27)$$

where J denotes the moment of inertia of the rotor mass, $Jd(2\omega_r/P)/dt$ is the inertia torque, T_{em} is developed electromechanical torque, T_{mech} is the mechanical load torque, T_d is the torque of viscous damping and entire expression on the right hand side of Eq. (27) means the accelerating torque. Mechanical load torque is positive in the motoring mode and negative in the generating mode of operation. Positive mechanical load torque in motoring mode decreases the accelerating torque and reduces the normalized angular speed of the rotor, while the negative mechanical load torque in generating mode increases the accelerating torque and causes the rotor angular speed to exceed the synchronous angular speed.

3 Dynamic simulations of drives with induction machines in Mathematica®

Dynamic simulations of drives with induction machines are performed in the programming environment Mathematica® in stationary reference frame. The mathematical model of simulations therefore consist of six voltage ODE's of the first order, that is of Eqs. (25) and (26), of the magnetic linear, algebraic flux linkage per second equation (23), of the developed electromechanical torque equation (24) and of the torque balance equation (27). In the sequel, the motoring, generating and braking modes of operation of electric motor drives with the induction machine are analyzed. The same machine is used in all operation modes, where its parameters

used in simulations are: the rated power of the three-phase, four pole machine is S_b=750 W, the rated phase-to-phase rms voltage is V=200 V, the rated frequency is f=50 Hz and the moment of inertia of the rotor mass is J=0.1 kgm^2. The ohmic resistances and reactances of single stator winding are r_s=3.35 Ω and x_{ls}=2.18 Ω, respectively. The values of ohmic resistance and reactance of a single phase rotor winding are recomputed to the stator and denoted by primes. These values are r'_r=1.99 Ω and $x'_{lr}=x_{ls}$=2.18 Ω, respectively. The value of magnetizing reactance is chosen to be x_m=51.44 Ω. All dynamic simulations are performed in the time interval, which lasted between 0 s and t_{final}=2 s.

3.1 Electric motor drive in motoring mode of operation

First dynamic simulation treats electric motor drive in motoring mode of operation, where the induction machine is loaded by a time-variable mechanical torque. The time interval of simulation $0 \le t \le t_{final}$ is divided into four subintervals, each of its is lasting for 0.5 s. In the first subinterval $0 \le t \le 0.5$ s, the electric motor is'nt loaded, while in the subinterval 0.5 s$\le t \le$1.0 s is loaded by the half of the base torque $0.5 T_b$, where the base torque is equal to $T_b=S_b/\omega_{bm}=(P\ S_b)/(2\ \omega_b)$. In the third subinterval 1.0 s$\le t \le$1.5 s, the electric motor is fully loaded by the base torque T_b, however in the last subinterval it is relieved with the half base torque.

The Fig.3 presents the dynamical response of the developed electromechanical torque of undamped as well as viscously damped drive in motoring mode. On the Fig. 3a it is shown, that electromechanical torque of the undamped drive, drawn by the solid line, after the transient period approaches to the value of the mechanical load torque. The electromechanical torque of the viscously damped drive, drawn by dashed line after the transient period takes higher values, because it must balance the sum of the mechanical load torque plus the damping torque. The damping torque is modeled by relationship $T_d=c(\omega_r/\omega_b)$, where damping coefficient takes the value.c=0.75 Nm. The Fig. 3b presents the dynamic response of the electromechanic torque as a function of the normalized rotor angular speed in both undamped as well as viscously damped drive.

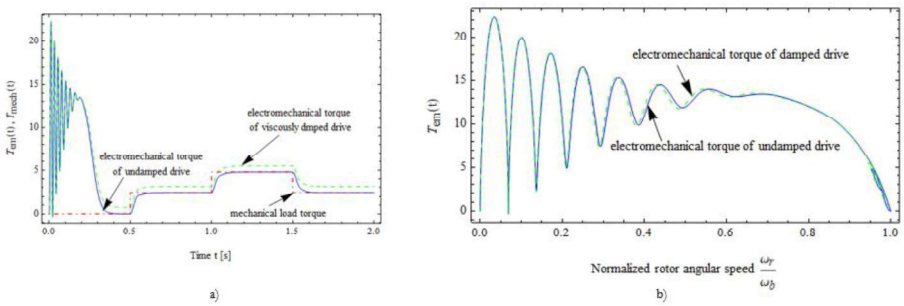

Figure 3: Electromechanical torque of the drive in motoring mode of operation. a) time response of the electromechanical torque, b) torque curve in dependence of the normalized rotor angular speed. Source: own.

In the Fig. 4, the time course of normalized rotor angular velocity is shown, where we can see that the normalized rotor angular velocities of the viscously damped drive differ very little from the normalized rotor angular velocities of the undamped drive. Further, we clearly see that the normalized angular velocity of the rotor steeply increases during the start of the electric motor and decreases slightly in the time intervals in which the electric motor is mechanically more loaded. In addition, we see that in the motor mode of operation the normalized angular velocity of the rotor never exceeds the value 1.

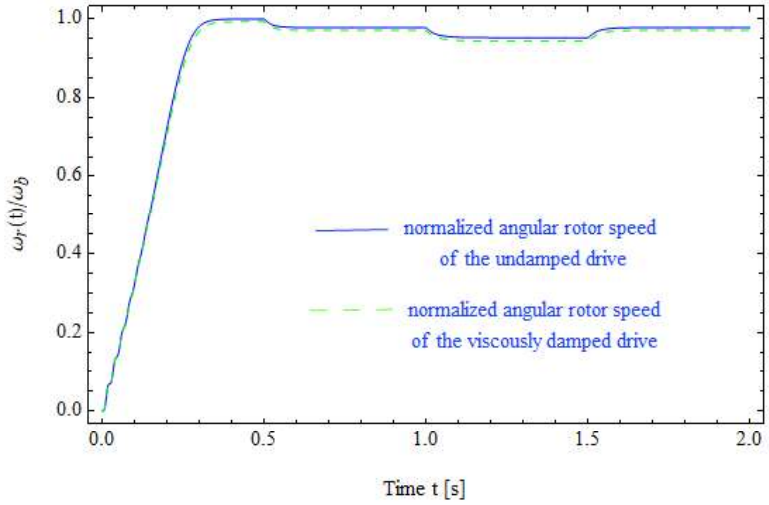

Figure 4: Time course of the normalized angular velocity of the rotor during motoring mode of operation. Source: own.

In the Fig. 5a, the time response of the stator current $i_{qs}(t)$ is shown in $qd0$ variables and in the Fig. 5b, the corresponding time response of on the stator recomputed rotor current $i'_{qr}(t)$ in $qd0$ variables is presented. From both figures it can be concluded that during the start of the machine, a strong transient phenomenon occurs with high amplitude oscillations. During the time subintervals in which the machine is gradually mechanically more loaded, a corresponding increase in the amplitudes of both currents can be observed. The responses shown in Figs. 5a,b refer only on the undamped drive.

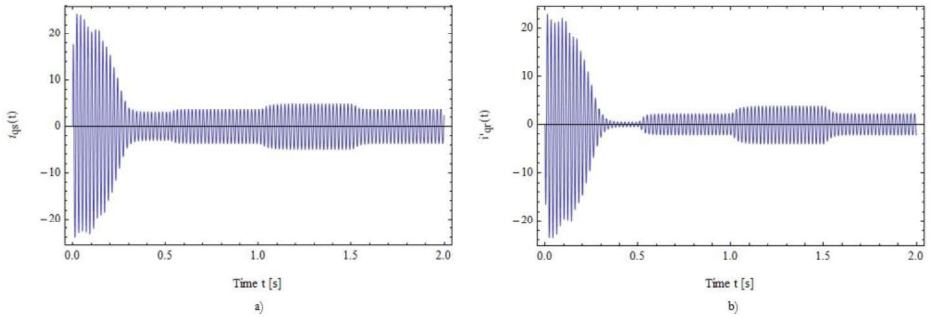

Figure 5: Time responses of a) the stator current $i_{qs}(t)$ and b) on the stator recomputed rotor current $i'_{qr}(t)$ in $qd0$ variables. Source: own.

3.2 Electric motor drive in generating mode of operation

The second simulation treats the electric motor drive with same machine data operating in the generator mode. To enable such operation, the mechanical load torque must be negative such that there is a net positive acceleration torque, which causes the increase of the rotor angular speed over the value of the synchronous angular speed or the increase of the normalized rotor angular speed over the value 1, respectively. To satisfy such a requirement, the time course of the mechanical load torque is changed in this simulation and is divided into two subintervals, where in the first subinterval $0 \leq t \leq 1.0$ s the electric motor is'nt loaded and in the second subinterval $1.0 \leq t \leq t_{final} = 2$ s it is loaded by the mechanical torque $-0.5T_b$. The effect of the viscous damping is not studied in this simulation. The time responses of the electromechanical torque in generator mode is plotted in the Fig. 6a, where we see that in the steady state of the second time subinterval the mechanical load torque is balanced with the driving torque because the drive is undamped. In the Fig. 6b it

can be seen that the normalized angular velocity of the rotor in the second time subinterval exceeds the value 1 as is expected.

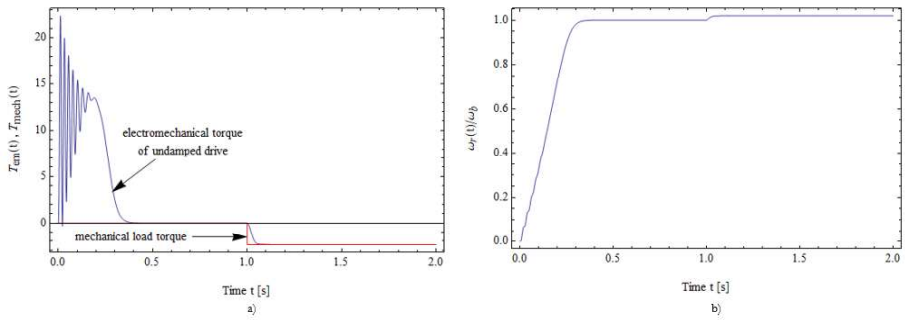

Figure 6: Time responses of electric motor drive in generating mode of operation. a) time response of the electromechanical torque, b) time response of the normalized angular velocity of the rotor. Source: own.

3.3 Electric motor drive in braking mode of operation

The third simulation treats the electric motor drive with same machine data operating in the braking mode. The braking mode of an electric motor drive can be simulated by reversing the direction of rotation of the rotating magnetic field, which is produced by currents in the stator windings that are 120° out of phase with each other. This can be achieved if two phases of the supply voltages are interchanged. In the simulation, the electric motor again is'nt loaded during the first time subinterval $0 \leq t \leq 1.0$ s and then in the second subinterval $1.0 \leq t \leq t_{final}=2$ s it is loaded by the mechanical load torque T_b. The interchange of terminals of two phase voltages is performed in the time $t=1$ s, when the electric motor starts to brake.

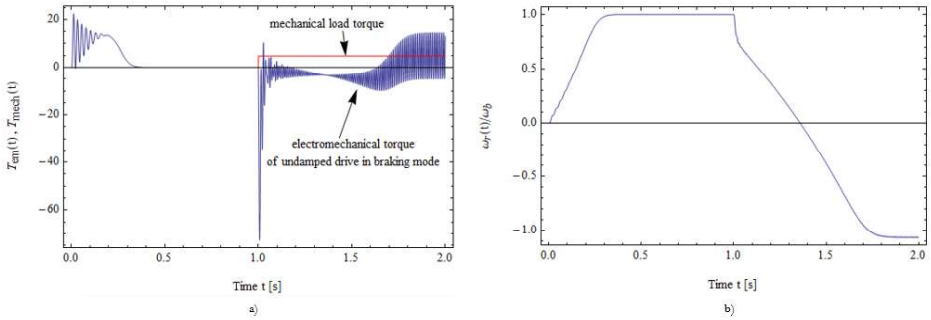

Figure 7: Time responses of electric motor drive in braking mode of operation. a) time response of the electromechanical torque, b) time response of the normalized angular velocity of the rotor. Source: own.

The time responses of the electromechanical torque and of the normalized angular velocity of the rotor, respectively in the braking mode of the electric motor drive are shown in the Fig. 7. It is evident, that due to the same operating conditions as are prescribed in generator mode for the first time subinterval, the course of the electromechanical torque in Fig. 7a is similar to the plot, depicted in Fig. 6a. However, as the braking starts in the time t=1 s, the electromechanical torque begins to strongly oscillate. In accordance with the signs of torques on the right hand side of Eq. (27), the net negative acceleration torque is produced for the most of the second time subinterval, which causes the decrease of the normalized angular velocity of the rotor. The value of the normalized rotor angular velocity ω_r/ω_b in Fig. 7b first decreases to zero and then becomes negative, indicating that the rotor begins to rotate in the opposite direction. Lastly, the angular velocity of the rotor approaches to reach the limit value of negative base angular velocity $-\omega_b$, which corresponds to the value of the normalized angular velocity of the rotor ω_r/ω_b = -1, as shown in Fig. 7b.

4 Conclusions

The mathematical model in the stationary reference frame, implemented in the programming environment Mathematica® is developed for dynamical simulations of the electric motor drives with three-phase induction machines. In the model, magnetically linear machine is treated. By using symbolic computing in the software system, the governing equations of the induction machine are derived, which saves extensive manipulative work. The developed mathematical model is succesfully applied in simulations of electric drives, operating in the motoring, generating and braking mode. The presented model can be upgraded to treat magnetically nonlinear induction machines as well as to couple the sophisticated mechanical assemblies [3].

References

Abouzeid, A. F., Guerrero, J. M., Endemaño, A., Muniategui, I., Ortega, D., Larrazabal, I. and Briz, F. (2020). Control Strategies for Induction Motors in Railway Traction Applications. *Energies, 13*, 700. doi:10.3390/en13030700

Heimann, B., Gert, W., Popp, K. (2007). Mechatronik: Komponenten, Methoden, Beispiele. *Carl Hanser Verlag München,* ISBN 3446405992

Kastrevc, M., Pušenjak, R. (2005). Fuzzy pressure control of hydraulic system with gear pump driven by variable speed induction electro-motor. *Experimental techniques*, *29*(*3*), 57-62.
Merve, S. K. (2023). The Use of Induction Motors in Electric Vehicles. In book: Induction Motors-Recent Advances, New Perspectives and Applications. Doi: 10.57772/*Intechopen.* 1000865